Magnetohydrodynamics of stably stratified regions in planets and stars

J. Philidet, C. Gissinger, F. Lignières, L. Petitdemange

Magnetohydrodynamics of stably-stratified conducting regions in planets and stars

J.Philidet†, C.Gissinger‡, F.Lignières§ and L.Petitdemange* ¶

† LESIA, Observatoire de Paris, PSL Research University, CNRS

Marie Curie, Université Paris Diderot, 92195 Meudon, France

‡ Laboratoire de Physique Statistique, Ecole Normale Superieure, CNRS , 24 rue Lhomond, 75005

§ CNRS, IRAP, 14 avenue Édouard Belin, 31400 T oulouse, France

¶ LERMA, Observatoire de Paris, PSL Research University, CNRS, Sorbonne Universités, UPMC

Univ. Paris 06, Ecole Normale Supérieure, 75005 Paris

October 30, 2019

Abstract

Stably-stratified layers are present in stellar interiors (radiative zones) as well as planetary interiors (recent observations and theoretical studies of the Earth's magnetic field seem to indicate the presence of a thin, stably-stratified layer at the top of the liquid outer core). We present direct numerical simulations of this region, which is modeled as an axisymmetric spherical Couette flow for a stably-stratified fluid embedded in a dipolar magnetic field. For strong magnetic fields, a super-rotating shear layer, rotating nearly 40% faster than the inner region, is generated in the stably stratified region. In the Earth context, and contrary to what was previously believed, we show that this super-rotation may extend toward the Earth magnetostrophic regime if the density stratification is sufficiently large. The corresponding differential rotation triggers magnetohydrodynamic instabilities and waves in the stratified region, which feature growth rates comparable to the observed timescale for geomagnetic secular variations and jerks. In the stellar context, we perform a linear analysis which shows that similar instabilities are likely to arise, and we argue that it may explain the observed magnetic desert among massive and intermediate mass stars.

1 Introduction

Understanding the origin of the diversity of stellar magnetic fields is a research topic in which important advances have been recently made and much more are expected soon. This topic is pushed by new observations of ground-based instruments, in particular spectropolarimeters, as well as observations

---

**Corresponding author. Email: ludovic@lra.ens.fr

from space (with Corot and Kepler for instance). It also benefits from the results of simulations which, thanks to the numerical resources now available and the progress of astrophysical modeling, allow us to study the complex physics of stellar interiors taking into account many effects such as rotation, magnetism, turbulence... Until recently, only the Sun was accessible to us; now, stellar physics has become a privileged laboratory for deepening our knowledge of different aspects of fundamental physics. It is one of the few themes in astrophysics in which advanced theories can be directly confronted with observational constraints. However, although it is accepted that magnetism can play a major role in most stages of a star life, its effects are mainly ignored in stellar evolution codes (in particular unidimensional codes in which most physical effects are simply parametrised). Taking into account these magnetic effects is one of the major current issues in astrophysics.

Stellar magnetic fields can be classified into two broad categories. In the first category, magnetic fields are generated and maintained by convective motions in deep layers, through what is referred to as dynamo effect. There are countless different mechanisms through which dynamo can give rise either to stationnary fields, large-scale dipoles like those observed for rapidly rotating low-mass, M type stars, or to time-dependent fields. The periodic variation of the solar field has been observed since Galileo through the counting of solar dark spots. For these stars having masses less than or equal to those of the Sun, dynamo mechanisms seem to be very efficient in their thick convective zone, an idea supported by many studies on planetary magnetism [Roberts and King, 2013, Petitdemange, 2018]. In the second category, on the other hand, massive stars harbor strong dipolar fields with a stable configuration, commonly referred to as "fossil fields", for it has been established that it results from the formation of the star. Unlike dynamo-driven fields, the origin of magnetism in stars possessing a thick radiative zone located on the top is poorly explored by theoretical studies, and understanding it remains a major challenge.

Thanks to the improved sensitivity of a new generation of spectropolarimeters, the existence of a dichotomy in the magnetic field amplitudes for massive and intermediate mass stars is now clear [Lignières et al., 2014]. Indeed, the observations show a large gap between strong fields (fossil fields with amplitudes above 300 G) and fields of ultra-weak, sub-gauss magnitude. This gap, referred to as the "magnetic desert", stretches over two orders of magnitude. Massive and intermediate mass stars have a thick radiative zone above a small convective zone (see Braithwaite and Spruit [2017] for a review). Therefore, to understand these observations, we need to both determine how strong magnetic fields can be maintained on long time scales in their radiative zone, and at the same time study the processes of saturation of dynamos from shear flows in radiative zones, that is in stably stratified environments.

After its exponential growth phase, the dynamo-generated magnetic energy can indeed saturate to a level sufficiently high to affect the flow. It is well known that the magnetic tension significantly reduces the differential rotation. One of the complexities of magnetohydrodynamic (MHD) processes is the strongly nonlinear character of the retroaction, through the Lorentz force, of the magnetic

2

field on the flow that initially amplified it. Differential rotation and magnetism thus appear as intimately linked phenomena. Differential rotation, by itself or by developing hydrodynamic instabilities, can generate dynamo-generated fields, and this magnetism can inhibit these instabilities or even greatly reduce the differential rotation by transporting angular momentum outward. This last process could explain the magnitude of the differential rotation observed by asteroseismology for different stars [Deheuvels et al., 2014, Triana et al., 2015]. According to Fossat et al. [2017], a strong shear layer could be present in the solar radiative zone.

MHD phenomena are crucial to the understanding of planetary interiors as well. The Earth magnetic field is known to be generated by dynamo effects taking place in its liquid outer core. The study of this region in the scope of MHD may therefore give some insight into the variations of the Earth magnetic field. Those take place on time scales ranging from less than a year to millions of years. In particular, the variations of the length of day on timescales ranging from 1 to 100 years are believed to be caused by geomagnetic fluctuations featuring these typical periods, so called secular variations (SV). However, while being observed for a long time and monitored with an ever increasing accuracy [Chulliat and Maus, 2014, Chulliat et al., 2015, Finlay et al., 2016], geomagnetic variations remain a fascinating problem as several features of the so-called magnetic jerks are still unclear. In particular, it was recently suggested [Buffett et al., 2016] that the presence of a certain type of MHD waves resulting from the interaction between magnetic tension, Archimedes force and Coriolis force in a 140 km thin stably-stratified layer located at the top of the Earth's liquid outer core [Braginsky, 1993] may account for unexplained secular fluctuations of the geomagnetic dipole field. The presence of this layer at the core-mantle boundary (CMB) is believed to be due to the diffusion of light elements from the mantle to the core driven by mere pressure gradients [Gubbins and Davies, 2013].

Among the impacts a magnetic field can have on a flow embedded in it, one is the development of MHD instabilities. Under the conditions existing in a stellar radiative region, three main types of instabilities are likely to occur, which differ by the source of free energy they derive from. Gravitational energy can be released through Parker-like instabilities [Parker, 1966], magnetic free energy through purely magnetic instabilities (like the Tayler instability [Tayler, 1973] or induced by a gradient of toroidal magnetic field lines [Acheson and Hide, 1973]) while shear instabilities (like the magneto-rotational instability MRI or strato-rotational instability SRI) depend on the free kinetic energy in the differential rotation [Balbus and Hawley, 1991, 1998, Menou et al., 2004] for the MRI and Shalybkov and Rüdiger [2005] for the SRI). Differential rotation can also result from baroclinicity as shown by Rieutord [2006] who considered a Boussinesq model of a radiative envelope. In the simulations presented in this paper, these hydrodynamic or MHD instabilities are not taken into account as we focus here on the low Rossby number regime in which an axisymmetric steady state configuration exists. We postpone the numerical study of three dimensional structures induced by a strong differential rotation to a future paper. We only

3

argue on the possible development of MHD instabilities by means of analytical developments.

In this paper, we therefore propose a direct, global numerical modeling of stably stratified layers, by taking into account both the rotational influence of neighboring layers and the effect of the magnetic field generated in the conducting convective zone, and use this model to describe both the stably-stratified layer at the Earth CMB and stellar radiative zones. We present the numerical model in section 2; in section 3 and 4, we discuss the steady-state flow configuration yielded by these simulations. We show the influence of rotation and stratification on the geometry of the flow in purely hydrodynamical models in section 3 and we focus on the development of super-rotation induced by the combined influences of magnetism and stratification in section 4. In section 5, we perform a local, linear stability analysis to show that the combined effects of shear, magnetic field and stratification could yield MHD instabilities able to account for geomagnetic secular variations in the planetary context, or that they could affect the stability of dipolar fields observed for massive stars in the stellar context. We argue that this latter analytical result could explain the observed "magnetic desert" [Lignières et al., 2014].

2   Numerical model

In the present paper, we aim at modeling stably-stratified layers in the geophysical and astrophsyical contexts. In the planetary context, this corresponds to the 140 km thin shell located at the Core-Mantle Boundary (CMB), between the fluid, convective dynamo region and the solid mantle. In the stellar context, it corresponds to a radiative zone (more precisely a radiative envelope in the case of a massive or intermediate mass star). In both cases, the region that is being modeled is located between two spheres, and the aspect ratio in these two situations is drastically different (the planetary case is in the thin gap limit, whereas the stellar context is in the thick gap limit). It is important to stress out that a 3D modeling of such a flow would be extremely time-consuming when it comes to use parameter values relevant to both regimes. In particular, the Ekman number E, which measures the ratio between the viscous force and the Coriolis force, is close to $E \sim 10^{-15}$ in both cases, whereas classical DNS can only reach $E \gtrsim 10^{-7} - 10^{-8}$ [Schaeffer et al., 2017]. Furthermore, while classical models are essential to understand the evolution of magnetic fields on the magnetic dissipation time scale (about 10000 years), they are less suitable to the study of much shorter timescales (less than a century), such as we are here. For these different reasons, we use a more simplified approach, in which inertia (i.e advection terms) is neglected and axisymmetric calculations are performed, as described below.

The stably-stratified layer is therefore modeled as an axisymmetric spherical Couette flow embedded in a dipolar magnetic field. The inner sphere of radius r_i in which this magnetic field is generated represents the transition to the convective region in both contexts, and has the same conductivity as the modeled

fluid. The outer sphere of radius r_o, however, is insulating. In the planetary context, magnetic torques acting on the convective (inner) region make it rotate slightly faster than the outer, insulating sphere, such that a weak differential rotation (low Rossby limit) can develop in the stably stratified layer. In the stellar context, the rotation rate of the deeper convective region can increase during different phases of the star's likfe (see introduction). We model this by applying a slightly different rotation rate to the two shells, which will propagate to the fluid in between through no-slip mechanical boundary conditions. The calculations being performed in the frame of reference of the outer shell, the latter is motionless, whereas the inner shell has a slow rotation (compared to the global rotation of the frame of reference). Finally, a stable stratification is applied through a temperature difference between the inner and outer shells.

We consider the Boussinesq approximation, allowing us to neglect variations of the fluid density except in the buoyancy term, leading to the following dimensionless MHD equations :

$$
\begin{cases}
\dfrac{\partial \boldsymbol{v}}{\partial t} = & -(\boldsymbol{v}.\boldsymbol{\nabla})\boldsymbol{v} + E\Delta\boldsymbol{v} - 2\boldsymbol{e_z} \times \boldsymbol{v} - \boldsymbol{\nabla}P \\
& +\dfrac{E\Lambda}{Pm}(\boldsymbol{\nabla} \times \boldsymbol{B}) \times \boldsymbol{B} + E\widetilde{Ra}\Theta\boldsymbol{e_r} \\
\dfrac{\partial \boldsymbol{B}}{\partial t} = & \dfrac{E}{Pm}\Delta\boldsymbol{B} + \nabla \times (\boldsymbol{v} \times \boldsymbol{B}) \\
\dfrac{\partial T}{\partial t} = & -(\boldsymbol{v}.\boldsymbol{\nabla})T + \dfrac{E}{Pr}\Delta T
\end{cases}
\tag{1}
$$

where $\boldsymbol{v}$, P, $\boldsymbol{B}$ and T are the dimensionless velocity, pressure, magnetic field and temperature, Θ is the temperature fluctuation as a function of which we express the density fluctuations in the buoyancy term, $\boldsymbol{e_z}$ the unit vector representing the rotation axis and $\boldsymbol{e_r}$ the local radial unit vector. Time scales have been normalized by Ω_o^{-1} (rotation rate of the outer shell), spatial variables by the radius r_o of the outer sphere, the magnetic field by its amplitude B_o at $r = r_o$ in the equatorial plane and temperatures by the temperature difference ΔT between the shells. We introduce the following dimensionless numbers : the Ekman number $E = \nu/\Omega_o r_o^2$, the Elsasser number $\Lambda = B_o^2/\mu\rho\eta\Omega_o$ (ratio between the Lorentz force and the Coriolis force), the magnetic Prandtl number $Pm = \nu/\eta$, the (modified) Rayleigh number $\widetilde{Ra} = \alpha g\Delta T r_o/\nu\Omega_o$, the thermal Prandtl number $Pr = \nu/\kappa$ and the Rossby number $Ro = (\Omega_i - \Omega_o)/\Omega_o$. Following traditional notations, we denote the momentum diffusivity of the fluid as ν, its magnetic permeability as μ, its mean density as ρ, its magnetic resistivity as η, its thermal expansion coefficient as α, its thermal diffusivity as κ and the gravitational acceleration at the outer shell as g.

In order to carry out the study of this system, we follow what has been done in previous studies [Dormy et al., 1998, 2002] and consider a weak differential rotation, which corresponds to negligible non-linear terms. Thus, we have linearised Eq. 1 by expressing the magnetic field as $\boldsymbol{B} = \boldsymbol{B_o} + \boldsymbol{b}$ ($\boldsymbol{B_o}$ being a dipolar magnetic field, whose amplitude is controlled by Λ), the temperature as $T = T_s + \Theta$ (where T_s is the stationary solution to the heat equation without source $\Delta T_s = 0$), and by neglecting the advection term in the Navier-Stokes
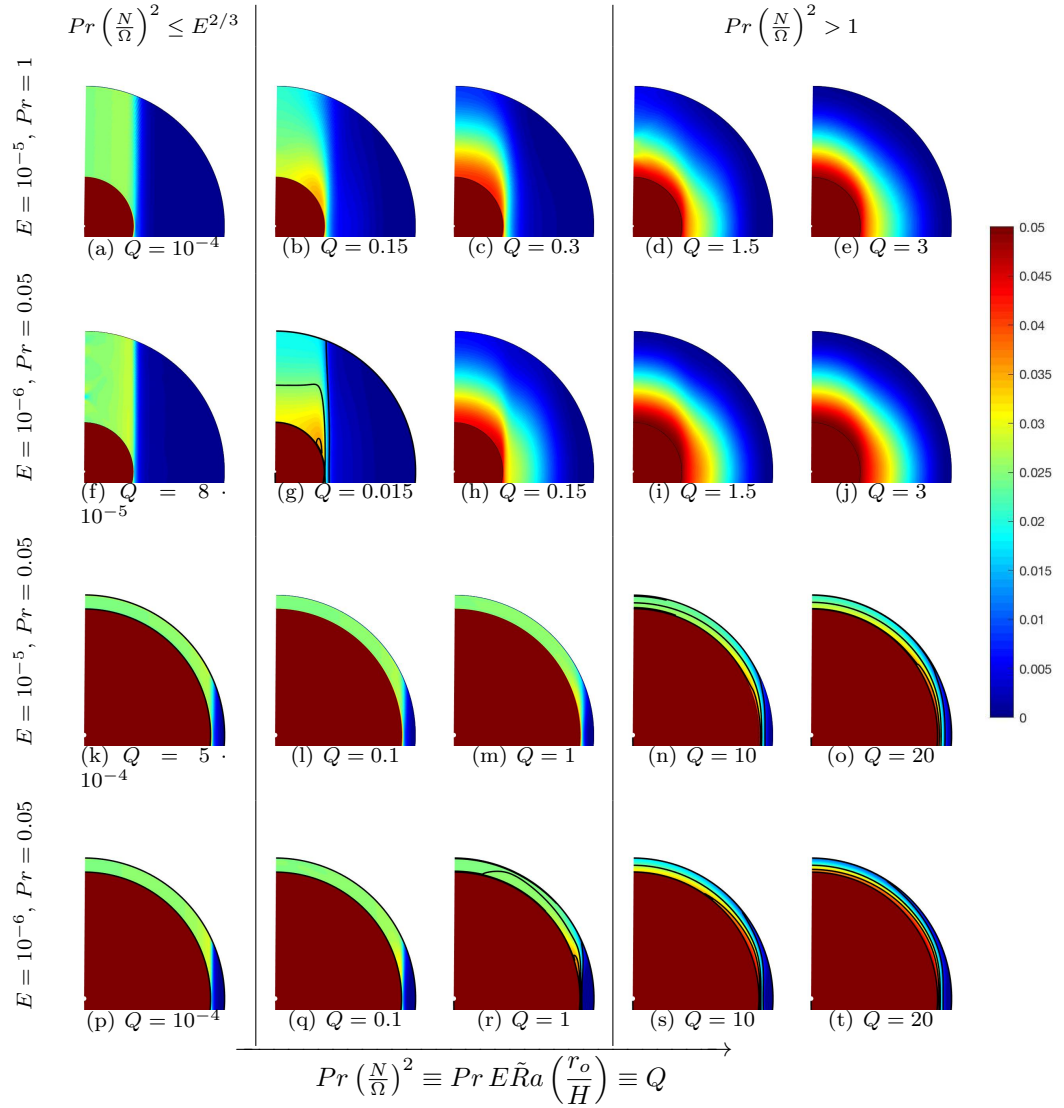
Figure 1: Rotation profile for purely hydrodynamic Couette flows with a weak differential rotation ($Ro = 0.05$) for different values of E and Pr, two different aspect ratios ($r_i/r_o = 0.35$ for the first two rows, 0.9 for the last two), as well as increasing values of Q (from left to right). As the amplitude of stratification is increased, the flow undergoes a continuous transition from cylindrical to spherical symmetry. The Earth's stratified layer lies in the intermediate regime, while the case of stellar radiative zones clearly lies in the spherically symmetric, high-Q regime. The solid black lines shown in non-trivial geometries are contours of equal rotation rate.

equation. We have then integrated these linearised equations using the PaRoDy code (Dormy et al. [1998] and later collaborations), over a time long enough to reach a stationary state. Note that compared to previous studies [Dormy et al., 1998, 2002], the novelty here lies in the introduction of stable stratification. Otherwise, we have followed their numerical method.

3 Hydrodynamical results and symmetry of the flow

We will discuss in detail the full MHD results in the next section; however, it is instructive to first describe the effect of a stable stratification on a spherical Couette flow in the purely hydrodynamical regime, that is with $\Lambda = 0$. Previous studies [Barcilon and Pedlosky, 1967a,b] investigated such an effect in a cylindrical geometry, and found that although the Rayleigh number and the Ekman number are independent control parameters, the structure of the flow is merely controlled by the value $Q \equiv Pr \left(\frac{N}{\Omega_o} \right)^2$ where N is the Brünt-Väisälä frequency. Using the dimensionless parameters introduced above, we can write $Q = Pr \times E \times \widetilde{Ra} \times \left(\frac{r_o}{r_o - r_i} \right)$ and by estimating $N^2 = \alpha g \Delta T / (r_o - r_i)$. In spherical shells, Garaud [2002] has studied the nonlinear problem by combining analytical and numerical developments, assuming axial symmetry of the problem and within some limits that are not considered here. Garaud [2002] has also noticed the important role of Q. We found a similar dependance with Q in our data. More precisely, 3 different regimes can be observed depending on the value of Q, as illustrated by Fig. 1 [Barcilon and Pedlosky, 1967a,b]. If $Q \ll E^{2/3}$ (left panels in Fig. 1), the flow is driven by Coriolis forces and exhibits a cylindrical geometry. On the other hand, if $Q \gg 1$ (right panels in fig 1), the flow is driven by buoyancy, and a spherical symmetry is observed for the flow. In between, neither one dominates the other. To draw fig 1, we have varied the value of Q by changing E, Pr and the aspect ratio. It is important to note that additional simulations (not shown) have been run with different parameters and also show that Q is the key parameter.

In the solar case, Spiegel and Zahn [1992] have also noticed that Q is an important parameter in their study on the thickness of the tachocline. Due to the smallness of Pr (less than 10^{-5} according to Dormy, E. and Soward, A. M. [2007] and Thomas and Weiss [2008]), Q would be of the order of 1 in the solar radiative zone. Observations of stellar rotation periods show that Ω can vary by several orders of magnitude [Donati and Landstreet, 2009] and the different regimes highlighted here are all relevant in the stellar context.

For the Earth case, Roberts and King [2013] have provided an estimate for the Prandtl number at $P_r = 0.1$. However, in the outer core, the kinematic viscosity and the thermal diffusivity are so low compared to inertia that turbulence can significantly increase their effective values (turbulent diffusivities) such that Pr may approach unity. Buffett et al. [2016] have argued on the possibility that
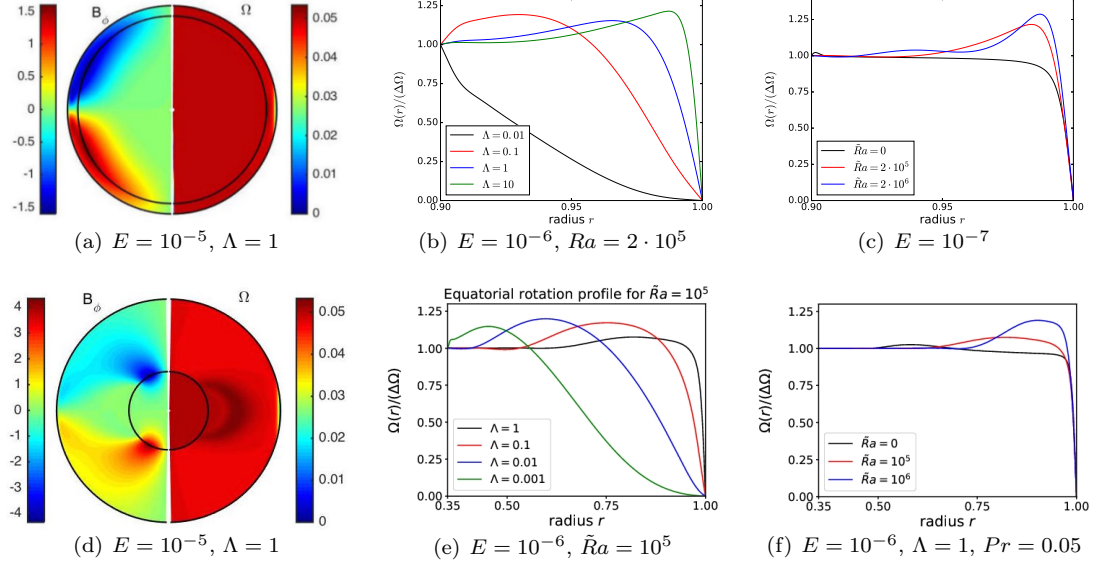
Figure 2: On the left (panel a, d) : Azimuthal magnetic field b_ϕ (left) and rotation profile (right) for $\Lambda = 1$, $R_o = 0.01$, $Pr = 0.05$ and $E = 10^{-5}$, for two different aspect ratios ($r_i/r_o = 0.9$ for the top row, 0.35 for the bottom row). Otherwise, equatorial rotation profile normalized by the differential rotation $\Delta\Omega$, shown for different values of Λ at $E = 10^{-6}$, $\widetilde{Ra} = 2 \cdot 10^5$, $Pr = 0.05$, (panel (b,e)), and for different values of $\widetilde{Ra}$ at $\Lambda = 1$, $Pr = 1$, $E = 10^{-7}$ (panel (c)). Regardless of the aspect ratio (thin gap on the top and thick gap on the bottom), super-rotation increases with both the magnetic field (Λ) and the stratification ($\tilde{Ra}$).

the buoyancy frequency $N = \sqrt{\alpha g \Delta T/H}$ may be comparable to the Earth rotation rate Ω_o. Consequently, the Rayleigh number would be linked to the Ekman number by the relationship $\widetilde{Ra}\, E \sim (r_o/H)$. In this case, the Earth would lie in the intermediate regime ($0.1 \lesssim Q_{\text{Earth}} \lesssim 1$), meaning that the rotation profile is unlikely to present a simple geometry ; furthermore, the Elsasser number for the Earth has a value close to $\Lambda_{\text{Earth}} \sim 1$, which means that the effects of the magnetic field are not negligible and can drastically change this geometry. (How about stars ?)

4   Super-Rotation induced by the combined influences of magnetism and stratification

We carry out the same direct numerical simulations (DNS) as presented in the previous section, but this time we add a dipolar magnetic field (thus

flows are no longer purely hydrodynamic). For the reasons we have developed above, non-linear terms in the set of equation 1 have been dropped altogether. We first show in the left panel of Fig.2 the rotation profile and corresponding azimuthal magnetic field for a flow where no stratification is applied. Note that the linearity of the equations implies that only the relative values for different regions make sense.

As illustrated by Fig.2-a, the structure of the flow is quite different from the hydrodynamic case, in which the rotation rate shows values halfway between that of inner and outer spheres. Here, the magnetic field lines corotate with the conducting inner core, and the magnetic torque naturally produces a co-rotation of the majority of the flow with the inner core, except at the outer boundary layer where viscosity effects are no longer negligible, and the no-slip condition makes the fluid corotate with the outer boundary. However, Fig.2-b shows that for sufficiently large magnetic field, part of the fluid located in the equatorial region rotates *faster* than the inner sphere. This phenomenon is commonly referred to as super-rotation [Dormy et al., 2002] and has been observed in both numerical simulations [Hollerbach et al., 2007] and experiments [Cardin and Olson, 1995] of magnetized spherical Couette flow. The mechanism involved is the following : since the magnetic field lines corotate with the conducting inner core, the bulk flow will therefore also corotate with it. So does the inner boundary layer, because the current can recirculate inside the conducting inner core there ; however, the insulating outer boundary layer can not, which means that the current cannot align with the dipolar magnetic field lines. It is therefore subjected to azimuthal Lorentz forces inducing an extra azimuthal velocity, that can be so high as to overcome the rotation rate of the core. This extra rotation rate propagates to the entire field line, thus explaining the characteristic crescent shape of the super-rotating regions.

Unfortunately, this fascinating phenomenon is known to vanish in presence of a strong global rotation [Dormy et al., 2002]. As shown in the following, it can however be restored in the presence of sufficiently large stable stratification, allowing super-rotation to play a role in the magnetostrophic regime relevant to the planetary context as well as the stellar context ($\Lambda \sim 1$, $R_o \ll 1$ and $E \ll 1$). Fig.2-c shows rotation profiles at the equator for $\Lambda = 1$ and different values of the Ekman number E. Regardless of the value of E, super-rotation increases as $\widetilde{Ra}$ increases and the super-rotating region migrates outward. As a result, we observe the emergence of a localized shear layer close to the CMB when the stratification is sufficiently high. Note that the position of the super-rotating region on the equator remains sensibly the same when $\widetilde{Ra}$ is increased, while its magnitude becomes larger.

Interestingly, the presence of stratification also strongly modifies the behavior of super-rotation in the limit of small Ekman number. Here we take the Earth context as an example : Fig.3-left shows the evolution of the rotation profiles with the global rotation for a given value of Q and Λ, which have been both fixed to their value expected for the Earth outer core, $Q \sim 2$ and $\Lambda \sim 1$. As the Ekman number is decreased, the super-rotating region is enhanced, suggesting a possible magnetostrophic super-rotation close to the CMB.
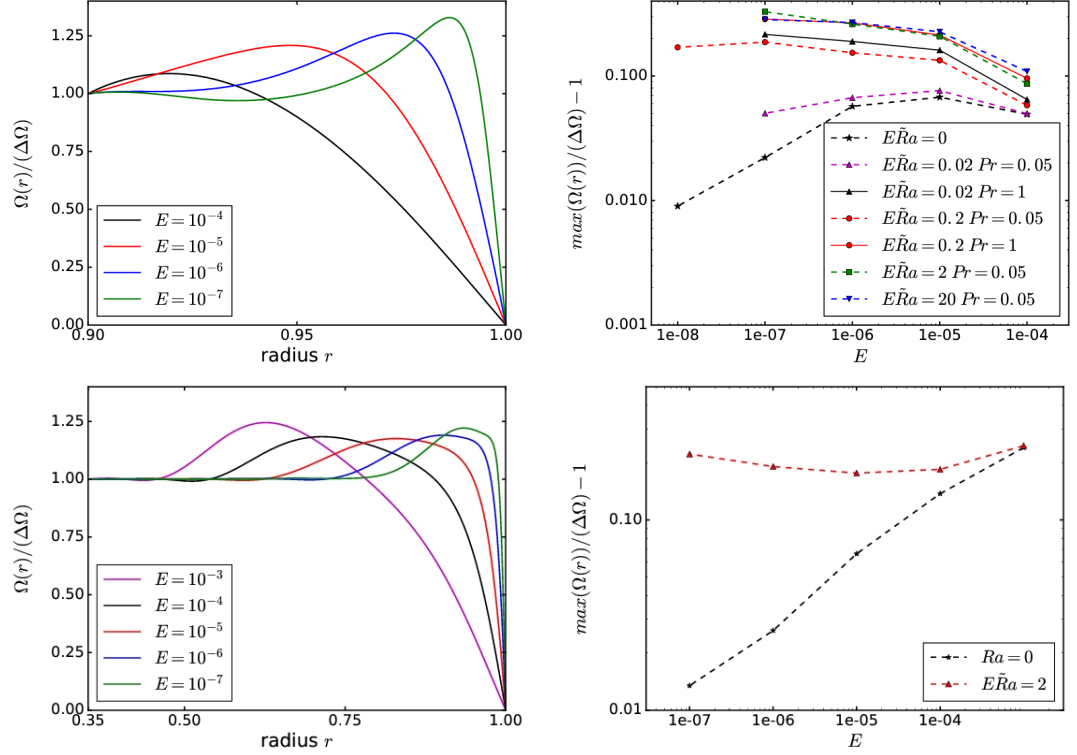
Figure 3: **Left** : equatorial rotation profiles for different values of E ($\widetilde{Ra} \times E = 2$, all other parameters same as Fig.1), showing the generation of a strong shear layer at low Ekman number. **Right** : Maximum amplitude of the equatorial angular velocity Ω_{max} normalized by the applied differential rotation $\Delta\Omega = \Omega_i - \Omega_0$ for different values of Pr and $E \times \widetilde{Ra}$, all other parameters same as Fig.1. Sufficiently large stratification leads to super-rotation independent of E at low Ekman number.

Precise values of Pr and $\widetilde{Ra}$ in the thin stably-stratified region of the Earth's outer core are still difficult to constrain, making very conjectural any prediction on the exact structure of such a shear layer. Still, the right panel of Fig.3 strengthens the idea that a super-rotating region similar to the one described here may be generated in this layer. Indeed, it shows that for sufficiently large stratification, the magnitude of the super-rotation seems to tend to a constant value in the magnetostrophic regime, independent of both the Ekman number and the dimensionless number Q.

These numerical simulations therefore suggest that the stably-stratified layer in the Earth outer core might be characterized by a super-rotating region in which the fluid could rotate up to 30% faster than the inner core. Because this mechanism is associated with a strong differential rotation, it provides a

simple source for the generation of the MAC waves generally invoked to account for some of the secular variations of the geomagnetic field. Below, we show that in addition to such waves, the stably-stratified layer can also be prone to MHD instabilities evolving on time scales similar to the Earth's magnetic secular variations.

5   Local description of unstable MHD modes

As pointed out above, the presence of stratification may strongly enhance the differential rotation, and leads to very localized shear through the generation of so-called super-rotation. The purpose of the present section is precisely to investigate the waves and instabilities prone to be generated in the stably-stratified layer whereas previous linear studies have ignored either the effects of differential rotation [Buffett et al., 2016] or the effects of stratification [Petitdemange et al., 2013] in the planetary context. In the stellar context, our stability analysis is strongly inspired by Menou et al. [2004]. By using recent observational constraints and a simpler linear analysis, we argue on the generation of unstable modes and their possible influences.

Because of the force balance achieved between the Lorentz, Coriolis and Archimedes forces, one expects so-called MAC waves to propagate in the stably-stratified layer, in addition to Alfvèn waves, purely hydrodynamic waves or torsionnal oscillations. Furthermore, in the presence of a weak magnetic field, a differentially rotating, conducting fluid can enter an unstable regime and develop what is refered to as the MagnetoRotationnal Instability (MRI). It is essential, for instance, to the understanding of the dynamics of accretion disks owing to the presence of a strong shear in these objects [Balbus and Hawley, 1998]. Although rotation properties of planetary interiors obviously differ from those of an accretion disk, it was also shown to be impacted by this instability [Petitdemange et al., 2008]. In this section, we study the possibility to see the MRI arise, and especially the impact of stratification and differential rotation on this instability, in two different contexts : planetary CMB and stellar radiative envelopes. In particular, this study stands out in that it extends earlier studies [Petitdemange et al., 2008] to account for the influence of stratification, which had not been accounted for before. Linear calculations show that stratification increases the threshold of the centrifugal instability. However, stable stratification acting on a differentially rotating fluid allows the development of the so-called StratoRotational Instability (SRI), which amplifies non-axisymmetric modes [Molemaker et al., 2001]. It was studied numerically [Shalybkov and Rüdiger, 2005] and experimentally [Le Bars and Le Gal, 2007]. The SRI has no effect on axisymmetric modes.

We follow the linearisation of Eq. 1 we have used in section 3, but this time we restrain ourselves to a local analysis and use the WKB approximation to extract a dispersion relation. We place ourselves near the equator where the magnetic field has no radial component. Ignoring the azimuthal component of the background magnetic field is not an important restriction as it is known that

the stability of axisymmetric MRI modes are not influenced by this component [Balbus and Hawley, 1998]. In addition, this azimuthal component has to match zero at $r = r_o$ as the outer shell is insulating in our model. Consequently we are left with the vertical component of $\boldsymbol{B_0}$ only. Consequently, the state around which we perform the linearisation is described by an azimuthal velocity field $\boldsymbol{V_0} = \Omega(s,z)s\boldsymbol{e_\phi}$ (with a rotation rate whose gradient we leave free), a uniform magnetic field $B_0\boldsymbol{e_z}$, and the stationary temperature $T_s(r)$ described in section 2. Note that in the Earth case, the thermal, momentum and magnetic diffusivities follow $\kappa \le \nu \ll \eta$, so that we may drop the thermal diffusivity κ (est-ce que c'est le cas dans les étoiles d'ailleurs ?). We find the following dispersion relation : $a_4\sigma^4 + a_3\sigma^3 + a_2\sigma^2 + a_1\sigma + a_0 = 0$ with :

$$
\begin{aligned}
a_4 &= \frac{k^2}{k_z^2} \\
a_3 &= 2\frac{k^4}{k_z^2}E_\eta + \frac{\widetilde{Ra}E}{k^2} \\
a_2 &= \frac{k^2}{k_z^2}(E_\eta^2 k^4 + 2\Lambda_m k_z^2) + 2\widetilde{Ra}EE_\eta - a \\
a_1 &= 2E_\eta\Lambda_m k^4 + E_\eta^2 E\widetilde{Ra}k^2 + \frac{\widetilde{Ra}E}{k^2}\Lambda_m k_z^2 - 2aE_\eta k^2 \\
a_0 &= \Lambda_m^2 k_z^2 k^2 + \widetilde{Ra}EE_\eta\Lambda_m k_z^2 - aE_\eta^2 k^4 - \Lambda_m k_z^2(a+4)
\end{aligned}
\tag{2}
$$

where

$$
a \equiv \frac{1}{s^3\Omega^2}\left(\frac{k_s}{k_z}\partial_z(s^4\Omega^2) - \partial_s(s^4\Omega^2)\right)
\tag{3}
$$

and $\Lambda_m = E\Lambda/P_m$, $E_\eta = E/P_m$, k_s and k_z are the nondimensionnalised radial and vertical component of the wavevector, and σ the nondimensionnalised complex growth rate of the spatial mode $\boldsymbol{k}$. This dispersion relation is compatible with the one obtained by Menou et al. [2004], where both their entropy dependent terms and the thermal diffusivity κ are neglected here. Note that, in the case of a purely radial differential rotation (as is the case locally near the equator), the parameter which we denote as a simplifies to $a = -4+2Ro'$ where the definition of the shear rate Ro' is based on the angular velocity jump $\delta\Omega$ over a characteristic length scale δs: $Ro' = (s/\Omega)\delta\Omega/(\delta s)$. We warn the reader that despite the fact they both measure differential rotation, the shear rate Ro' (which is a local quantity) is different from the Rossby number Ro introduced in section 2 (which is a global quantity).

5.1 The Earth case

The relevant force balance in the Earth core is the so-called MagnetoStrophic regime, which allows for the development of a slightly modified version of the classical MRI. We refer to this as the MagnetoStrophic-MRI, or MS-MRI [Petitdemange et al., 2008]. In particular, the differential rotation and the stable

stratification only play minor roles in this force balance. In this regime, a simpler (second order) dispersion relation can be obtained. Note that a similar dispersion relation can also be derived outside the magnetostrophic regime for a stably-stratified fluid in the special case where the eddy-diffusivities η and κ are equal :

$$4\Omega^2(\sigma + \eta k^2)^2 + \frac{k^2}{k_z^2}(k_z V_{Az})^4 + \alpha g \Delta T (k_z V_{Az})^2 + 2\Omega(k_z V_{Az})^2 s \frac{d\Omega}{ds} = 0 \quad (4)$$

where V_{Az} is the Alfvèn speed $V_{Az} = B_z/\sqrt{\mu\rho}$. The most unstable mode corresponds to a purely vertical one ($k_s = 0$), and its growth rate is :

$$\frac{\sigma_r}{\Omega} = \left(|Ro'| - \left(\frac{H}{r_o} \right) \widetilde{Ra}E \right) \frac{\Lambda/2}{1 + \sqrt{1 + \Lambda^2}} \quad (5)$$

This dispersion relation allows us to study the stability of a given mode, which we do in the following. In the Earth case, among the dimensionless parameters which play a role in the dispersion relation, several are fairly well constrained : we take $E \sim 10^{-15}$, $\Lambda \sim 1$ and $Pm \sim 10^{-5}$ (see Dormy, E. and Soward, A. M. [2007]). Both differential rotation and stratification however are poorly constrained, and as a result we keep Ro' and $\widetilde{Ra}$ free in the following. In Fig. 4, we have selected one spatial mode and studied both its stability and its oscillatory behaviour when differential rotation and stratification are changed.

When there is no stratification (left panel in Fig. 4), two different regimes can be extracted : if the shear rate is very low, the mode oscillates with a pulsation that is independent on Ro'. At higher Ro', however, the mode becomes unstable, and no longer oscillating. This is not surprising, as the differential rotation acts as a reservoir of energy for the MRI. Adding stable stratification (right panel in Fig. 4) decreases the growth rate of the instability in the unstable regime, especially for strong differential rotation. The purely oscillating, low-Ro' regime is replaced by a purely evanescent, non oscillating regime. Here, we see what equation 5 already taught us, that is stable stratification plays a stabilizing role for MS-MRI modes, in the sense that it suppress stable oscillations.

This local study also allows us to search for the most unstable spatial mode for a given set of dimensionless parameters. Figure 5 shows the evolution of the growth rate of the most unstable mode with the shear rate. In the left panel, we present the non-stratified case : the blue curve shows the numerical computation, with a low-Ro' regime where σ_r varies linearly with the shear rate, and a high-Ro' regime where σ_r varies with the square-root of the shear rate. We show the prediction from the magnetostrophic regime in orange, which we predictably retrieve for very low shear rates.

We show the stratified regime in the right panel. As we previously mentionned, stable stratification prevents the development of unstable modes at low shear rates. However, it leaves it unscathed when the differential rotation is stronger.

On a final note for the Earth case, we point out that for a shear rate of the order of several percents (which is the typical value obtained if the shear is
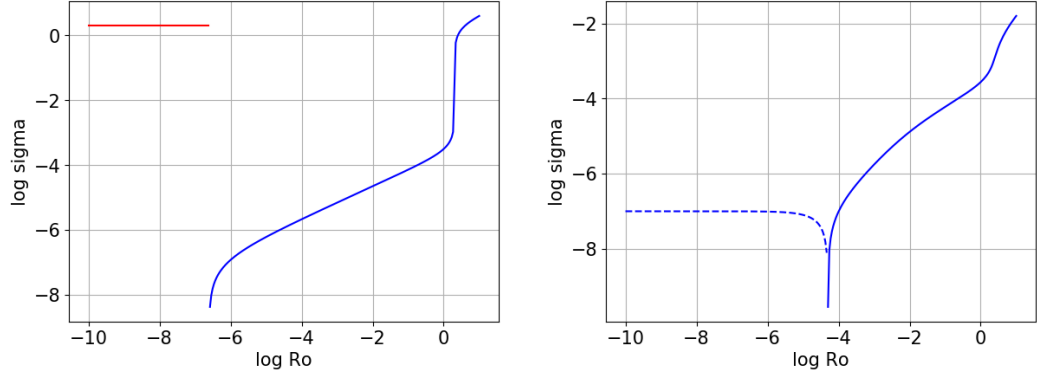
Figure 4: **Left** : Evolution of the growth rate σ of a given spatial mode with the shear rate Ro' ($E = 10^{-15}$, $P_m = 10^{-5}$, $\Lambda = 1$ and $\widetilde{R_a} = 0$). The blue curve shows the real part of σ when it is positive (i.e when the mode is unstable), the red curve shows the imaginary part of σ when it is non-vanishing. **Right** : Same as left panel, but with $\widetilde{R_a} = 10^{12}$. The graph solid blue line shows the real part of σ when it is positive, and the dashed blue line shows its opposite when σ_r is negative.
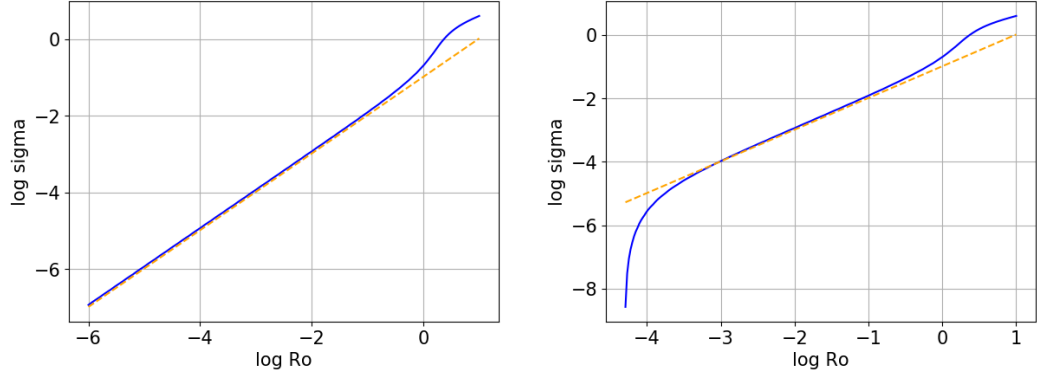

Figure 5: **Left** : Evolution of the growth rate σ of the most unstable mode with the shear rate Ro' ($E = 10^{-6}$, $P_m = 10^{-5}$, $\Lambda = 1$ and $\widetilde{R_a} = 0$). The orange curve shows the analytical solution that can be derived in the manetostrophic regime (equation 5). The blue curve shows the solution computed numerically.**Right** : Same as in the left panel, but with $\widetilde{R_a} = 10^{12}$.

14

due to super-rotation), and if we consider that stratification is not high enough to suppress the instability, the numerical study yields $\sigma_r \sim 10^{-3}$ in units of Ω_o, corresponding to a typical growth time $\tau \sim 3$ years, in agreement with the observed typical time scale for the Earth magnetic jerks.

5.2   The stellar case

The same dispersion relation can be used regardless of the context. However, the observational constraints are very different in the stellar case and in the Earth case, and we will therefore perform the analysis in the stellar case in a different fashion. In particular, following the stellar community, we prefer to describe the stratification with the Brunt-Väisälä frequency N rather than with the modified Rayleigh number, the two being linked *via* :

$$\left(\frac{N}{\Omega}\right)^2 = \frac{r_o}{r_o - r_i}\widetilde{Ra}E \tag{6}$$

As an example, we consider here the case of a star having just begun to climb the red giant branch (RGB). Due to the contraction of the core and the swelling of the enveloppe, we consider that the differential rotation is quite strong. Observational constraints indicate that the angular momentum is then redistributed throughout the star (see for instance Deheuvels 2014), thus damping the degree of differential rotation ; however, we place ourselves before the redistribution mechanism kicks in, and for illustrative purposes take $a \sim 1$ (which corresponds, for instance, to a keplerian rotation field). Furthermore, asteroseismic constraints also allow to probe the Brunt-Väisälä frequency in the interior of red giants, and give an estimate for the stratification. In particular, for a rapidly rotating red giant, we may take $N \sim \Omega$. Taking the Ekman number as $E \sim 10^{-15}$ (see Rincon 2019 again) then gives us an estimate for the Rayleigh number. Note to self : this entire paragraph must be burnt at all cost, and replaced by something that might possibly make sense instead.

We present in Figure 6 the results yielded by the dispersion relation 2 in this stellar case. The first three panels show the phase diagram of the system stability in the (Pm, Λ) plane for different amplitudes of the stratification. The non-stratified case (top-left panel in figure 6) yields a phase diagram that is well-known : there is a $Pm_{\min}$ below which the instability does not arise, and above that critical value one can see that the system is only unstable if Λ is in a certain window, whose width increases with Pm. The other panels show that, as we previously encountered with super-rotation, stable stratification has a stabilizing effect on the flow, in the sense that the unstable domain shrinks when $\widetilde{Ra}$ is increased. Note that in order to find the most unstable modes, we have arbitrarily restrained the search to spatial modes comprised between 10^{-7} and 10^7 in units of the radius gap H between the two shells, for both the radial and vertical component. This was done with the understanding that wave vectors whose norm is below 10^{-7} are bigger than the system itself, rendering this local analysis invalid, and that wave vectors whose norm is above 10^7 are killed
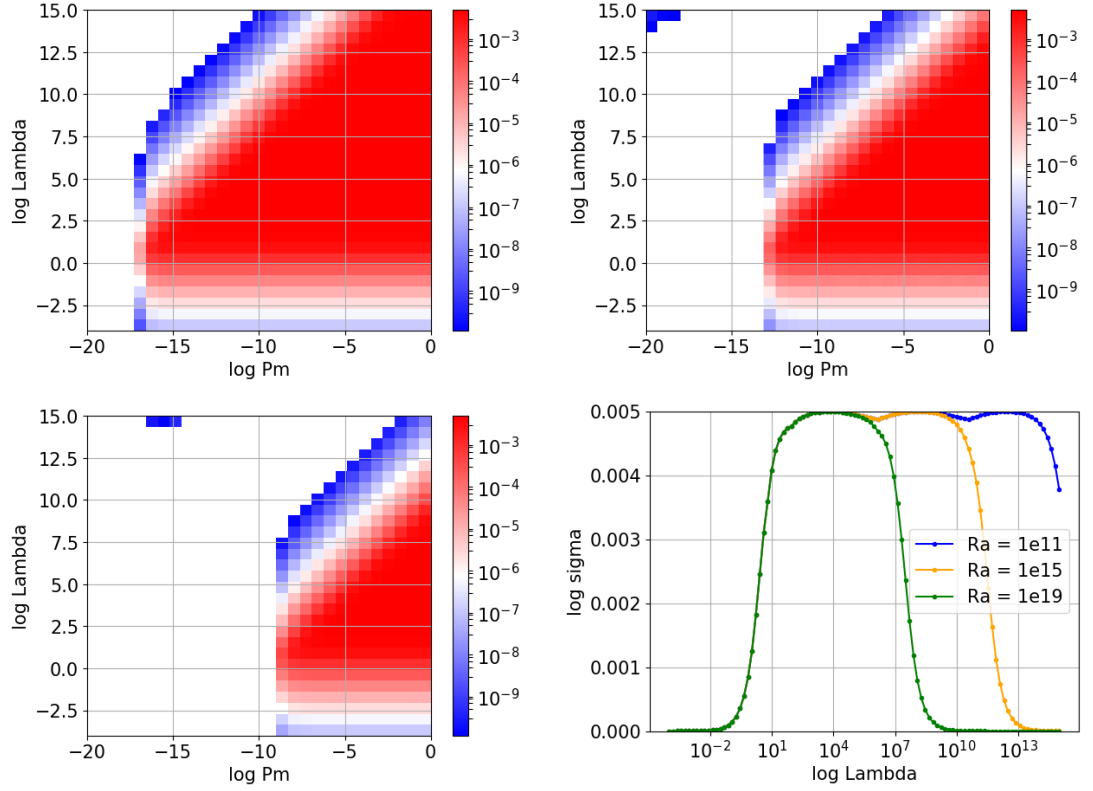
Figure 6: **Top left :** Phase diagram of the flow stability in the $(\log \Lambda, \log P_m)$ plane, for $E = 10^{-15}$, $Ro' = 0.01$ and $E \times \widetilde{Ra} = 10^{-4}$. The color bar shows the growth rate of the most unstable spatial mode (logarithmic scale) when it exists. The white zones on the left hand side of the phase diagram corresponds to the stable domain. **Top right :** Same with $E \times \widetilde{Ra} = 1$. **Bottom left :** Same with $E \times \widetilde{Ra} = 10^4$. **Bottom right :** Evolution of σ_r with Λ, for the same parameters as the three other panels, $Pm = 10^{-2}$ and different values of $\widetilde{Ra}$, showing that the unstable Λ-window shrinks as the amplitude of stratification is increased.

by dissipative effects. Therefore, while the dispersion relation always formally produce unstable modes regardless of the value taken by the dimensionless parameters, there is a domain, drawn in white in Figure 6, in which the only unstable spatial modes are not physically meaningful.

In the last panel of Figure 6 we present a vertical cut of the other panels at $Pm = 10^{-2}$, which corresponds to the value of the magnetic Prandtl number at the top of the Sun radiative core for instance. One can clearly see that the instability window shrinks with increasing stratification. The typical growth rate of the instability within the window remains, however, independent from the stratification.

The results presented above support the idea that, in the parameter range relevant to the context of stellar radiative zones, the MRI is indeed likely to arise, but only if the magnetic field lies in a certain range. Therefore, the MRI may provide a viable mechanism to explain magnetic desert among intermediate mass stars. Indeed, if the magnetic field harbored by the star during the early phases of its life has a high enough amplitude, it will prevent this instability from developing, and the star will continue to feature this fossil field. Otherwise, the MRI can develop, and its saturation will destroy the magnetic field that generated it. Alone would survive the magnetic field generated by dynamo effect in the convective zone of the star; given the small size of said region, the surviving field will be much lower than the original field, and may not be subjected to the MRI. As a result, we propose the following picture of intermediate mass star magnetism : A_p/B_p magnetism is a result of fossil fields strong enough to prevent the MRI from developing; and in Vega-like magnetism the fossil field has been destroyed by MRI, thus letting dynamo-generated fields dominate, which are too small to trigger the MRI. Note that, in regards to the magnetic instability windows shown in Fig. 6, its width in terms of Λ is twice that in terms of B_o, since $\Lambda \propto B_o^2$.

There is another type of stars in which differential rotation is of primary importance, and those are red giant stars. It is well known, indeed, that these stars feature a strong, localised shear layer near their H-burning shell [Deheuvels et al., 2014], which is however much weaker than predicted from theory or simulations (the shear rate Ro' inferred from observations is of order unity, while the predicted value would be of order 10^{2-3}). The MRI is likely to play a crucial role in the dynamics of such region; if that is the case, the saturation of this instability would, as we mentionned in the case of main-sequence, intermediate mass stars, destroy the flow configuration that allowed it to develop, thus smoothing differential rotation. Indeed, since the convective region in giant stars is much deeper than in intermediate mass stars, dynamo-driven magnetic fields may in this case resist the development of the MRI, and the flow would then be affected not through its magnetic field, but through its differential rotation. Therefore, it is possible that the MRI may play a role in the angular momentum transport needed to account for the observed rotation rate difference between the core and the enveloppe.

6 Summary and perspectives

In this study, we have modeled a stably-stratified region with an axisymmetric spherical Couette flow embedded in a dipolar magnetic field. We have split this study two ways, by applying this model to two different astrophysical objects : the thin, stably-stratified layer at the Earth CMB; and stellar radiative zones.

In the Earth context, the most striking feature is the generation of super-rotation in the limit $E \ll 1, \Lambda \sim 1$. Combined with MAC waves which are known to transport angular momentum in such a stably-stratified layer [Buffett et al., 2016], the magnetostrophic super-rotation can exert strong shear at the CMB. This new source of shear might be crucial for the understanding of some of the behavior of the Earth's magnetic field, such as the variations in the length of day, or the geomagnetic jerks. Indeed, our local analysis shows that the presence of strong enough shear at the Earth's CMB might trigger MHD instabilities. We showed that the stratification has little direct impact on the growth rate of such instabilities, which arises as long as $\widetilde{Ra}$ remains reasonably low. This suggests that such a flow is likely to be unstable as long as the amplitude R'_o of the differential rotation due to super-rotation remains close to the rough estimate $\sim 10^{-2}$. The stratification enables the presence of such a localized shear by restoring super-rotation (in the magnetostrophic regime) close to the CMB. In addition, the localization of super-rotation at the equator may explain why several magnetic features are mainly observed at very low latitudes (see for instance Chulliat and Maus [2014] and Finlay et al. [2016]). Furthermore, the observed variations in the length of day might be caused by an acceleration of the Earth's mantle due to the non-linear part of the instability. Finally, note that a non-axisymmetric model would be required to explain periodic local magnetic jerks [Petitdemange et al., 2013]. Further investigations on this matter would require a more in-depth study of non-axisymmetric modes in a stratified flow.

In the stellar context, we focused not so much on the possibility to see super-rotation arise from the interaction between differential rotation and magnetic field (such a shear structure may in this context be subject to large-scale flows, like meridional recirculation, which we have not taken into account) as we have on the potential instabilities which might dramatically affect the flow, in particular the MRI. We show here through a local linear analysis that in the parameter range relevant to the context of stellar radiative zones, the MRI is indeed likely to arise. One of the recognisable characteristic of this intability is that it requires the magnetic field amplitude to lie in a certain instability window. We show that stable stratification plays a stabilizing role with respect to the MRI, in the sense that it reduces this unstable window. While it may seem far-fetched to draw quantitative conclusions at this stage, we nonetheless propose a mechanism through which the MRI may explain the magnetic desert observed among intermediate mass stars.

The model we propose here is a simple one, and many aspects of the situation have been overlooked in the process. In particular, we have overly simplified the behaviour of the transition region between the convective interior and the

18

radiative enveloppe at radius r_i. While we have imposed a mechanical no-slip boundary condition there, it is well known that, because of inertia, the convective flow in the former overshoots in the latter. The radial velocity entailed by this mechanism thus have on the flow in the stably-stratified layer an impact that may be global; further studies will have to adress this point. Furthermore, it is natural that our axisymmetric study be extended to non-axisymmetric, tridimensionnal simulations, for a lot of instability mechanism in the studied contexts do not arise in axisymmetric environments. Finally, we have focused in this paper on the linear part of the instability, before its saturation. While we have strived to draw conclusions about the impact of the saturated phase on the flow, it will be necessary to study it numerically to confirm said conclusions. In particular, only then may the results obtained be quantitatively compared to observations.

Observations are indeed plentiful as far as this study goes. The Kepler mission has in particular given us access to extensive data on giant stars, thanks to which the issue of angular momentum redistribution can be studied in excruciating detail. Furthermore, concerning the intermediate mass stars magnetic desert, new observations of very young stellar objects may help us shed some light on the origin of magnetism in these stars, and in particular may help us to support the validity of the mechanism proposed in this paper. Tridimensionnal simulations are also crucial when it comes to understanding the origin of secular variations (SV) in geomagnetism, which are inherently non-axisymmetric. citer Olsen have investigated on the matter already, but in a parameter range that did not allow for the developement of the MRI. Performing a similar study with much lower Ekman number will allow for the study of the impact of this instability on the geomagnetic SV. The vastness of issues still open on the subject, as well as the innumerable observationnal data available to help solve them, mean that there is still a lot of work to be done.

Acknowledgments

References

D. J. Acheson and R. Hide. Hydromagnetics of rotating fluids. *Reports on Progress in Physics*, 36:159–221, Feb. 1973. doi: 10.1088/0034-4885/36/2/002.

S. A. Balbus and J. F. Hawley. A powerful local shear instability in weakly magnetized disks. I - Linear analysis. II - Nonlinear evolution. *Astrophysical Journal*, 376:214–233, July 1991. doi: 10.1086/170270.

S. A. Balbus and J. F. Hawley. Instability, turbulence, and enhanced transport in accretion disks. *Reviews of Modern Physics*, 70:1–53, Jan. 1998. doi: 10.1103/RevModPhys.70.1.

V. Barcilon and J. Pedlosky. Linear theory of rotating stratified fluid motions. *Journal of Fluid Mechanics*, 29(1):1–16, 1967a. doi: 10.1017/S002211206700059X.

V. Barcilon and J. Pedlosky. On the steady motions produced by a stable stratification in a rapidly rotating fluid. *Journal of Fluid Mechanics*, 29(4):673–690, 1967b. doi: 10.1017/S0022112067001119.

S. I. Braginsky. MAC-Oscillations of the Hidden Ocean of the Core. *Journal of Geomagnetism and Geoelectricity*, 45:1517–1538, 1993. doi: 10.5636/jgg.45.1517.

J. Braithwaite and H. C. Spruit. Magnetic fields in non-convective regions of stars. *Royal Society Open Science*, 4:160271, Feb. 2017. doi: 10.1098/rsos.160271.

B. Buffett, N. Knezek, and R. Holme. Evidence for mac waves at the top of earth's core and implications for variations in length of day. *Geophysical Journal International*, 204(3):1789–1800, 2016. doi: 10.1093/gji/ggv552. URL +http://dx.doi.org/10.1093/gji/ggv552.

P. Cardin and P. Olson. The influence of toroidal magnetic field on thermal convection in the core. *Earth Planet. Sci. Lett.*, 133:167–181, 1995.

A. Chulliat and S. Maus. Geomagnetic secular acceleration, jerks, and a localized standing wave at the core surface from 2000 to 2010. *Journal of Geophysical Research: Solid Earth*, 119(3):1531–1543, 2014. ISSN 2169-9356. doi: 10.1002/2013JB010604. URL http://dx.doi.org/10.1002/2013JB010604.

A. Chulliat, P. Alken, and S. Maus. Fast equatorial waves propagating at the top of the Earth's core. *Geophysics Research Letters*, 42:3321–3329, May 2015. doi: 10.1002/2015GL064067.

S. Deheuvels, G. Doğan, M. J. Goupil, T. Appourchaux, O. Benomar, H. Bruntt, T. L. Campante, L. Casagrande, T. Ceillier, G. R. Davies, P. De Cat, J. N. Fu, R. A. García, A. Lobel, B. Mosser, D. R. Reese, C. Regulo, J. Schou, T. Stahn, A. O. Thygesen, X. H. Yang, W. J. Chaplin, J. Christensen-Dalsgaard, P. Eggenberger, L. Gizon, S. Mathis, J. Molenda-Żakowicz, and M. Pinsonneault. Seismic constraints on the radial dependence of the internal rotation profiles of six Kepler subgiants and young red giants. *Astronomy and Astrophysics*, 564:A27, Apr. 2014. doi: 10.1051/0004-6361/201322779.

J.-F. Donati and J. D. Landstreet. Magnetic Fields of Nondegenerate Stars. *Annual Review of Astronomy and Astrophysics*, 47:333–370, Sept. 2009. doi: 10.1146/annurev-astro-082708-101833.

E. Dormy, P. Cardin, and D. Jault. MHD flow in a slightly differentially rotating spherical shell, with conducting inner core, in a dipolar magnetic field. *Earth Planet. Sci. Lett.*, 160:15–30, July 1998. doi: 10.1016/S0012-821X(98)00078-8.

E. Dormy, D. Jault, and A. Soward. A super-rotating shear layer in magnetohydrodynamic spherical Couette flow. *Journal of Fluid Mechanics*, 452:253–291, Feb. 2002. doi: 10.1017/S0022112001006711.

Dormy, E. and Soward, A. M., editor. *Mathematical aspects of natural dynamos*. CRC Press, 2007.

C. C. Finlay, N. Olsen, S. Kotsiaros, N. Gillet, and L. Tøffner-Clausen. Recent geomagnetic secular variation from swarm and ground observatories as estimated in the chaos-6 geomagnetic field model. *Earth, Planets and Space*, 68 (1):112, Jul 2016. ISSN 1880-5981. doi: 10.1186/s40623-016-0486-1. URL `https://doi.org/10.1186/s40623-016-0486-1`.

E. Fossat, P. Boumier, T. Corbard, J. Provost, D. Salabert, F. X. Schmider, A. H. Gabriel, G. Grec, C. Renaud, J. M. Robillot, T. Roca-Cortés, S. Turck-Chièze, R. K. Ulrich, and M. Lazrek. Asymptotic g modes: Evidence for a rapid rotation of the solar core. *Astronomy and Astrophysics*, 604:A40, Aug. 2017. doi: 10.1051/0004-6361/201730460.

P. Garaud. On rotationally driven meridional flows in stars. *Monthly Notices of the RAS*, 335:707–711, Sept. 2002. doi: 10.1046/j.1365-8711.2002.05662.x.

D. Gubbins and C. J. Davies. The stratified layer at the core-mantle boundary caused by barodiffusion of oxygen, sulphur and silicon. *Physics of the Earth and Planetary Interiors*, 215:21–28, Feb. 2013. doi: 10.1016/j.pepi.2012.11.001.

R. Hollerbach, E. Canet, and A. Fournier. Spherical Couette flow in a dipolar magnetic field. *European Journal of Mechanics B Fluids*, 26:729–737, Nov. 2007. doi: 10.1016/j.euromechflu.2007.02.002.

M. Le Bars and P. Le Gal. Experimental analysis of the stratorotational instability in a cylindrical couette flow. *Phys. Rev. Lett.*, 99:064502, Aug 2007. doi: 10.1103/PhysRevLett.99.064502. URL `https://link.aps.org/doi/10.1103/PhysRevLett.99.064502`.

F. Lignières, P. Petit, M. Aurière, G. A. Wade, and T. Böhm. The dichotomy between strong and ultra-weak magnetic fields among intermediate-mass stars. In P. Petit, M. Jardine, and H. C. Spruit, editors, *Magnetic Fields throughout Stellar Evolution*, volume 302 of *IAU Symposium*, pages 338–347, Aug. 2014. doi: 10.1017/S1743921314002440.

K. Menou, S. A. Balbus, and H. C. Spruit. Local Axisymmetric Diffusive Stability of Weakly Magnetized, Differentially Rotating, Stratified Fluids. *Astrophysical Journal*, 607:564–574, May 2004. doi: 10.1086/383463.

M. J. Molemaker, J. C. McWilliams, and I. Yavneh. Instability and equilibration of centrifugally stable stratified taylor-couette flow. *Phys. Rev. Lett.*, 86:5270–5273, Jun 2001. doi: 10.1103/PhysRevLett.86.5270. URL https://link.aps.org/doi/10.1103/PhysRevLett.86.5270.

E. N. Parker. The Dynamical State of the Interstellar Gas and Field. *Astrophysical Journal*, 145:811, Sept. 1966. doi: 10.1086/148828.

L. Petitdemange. Systematic parameter study of dynamo bifurcations in geodynamo simulations. *Physics of the Earth and Planetary Interiors*, 277:113–132, Apr. 2018. doi: 10.1016/j.pepi.2018.02.001.

L. Petitdemange, E. Dormy, and S. A. Balbus. Magnetostrophic MRI in the Earth's outer core. *Geophysical Research Letters*, 35:L15305, Aug. 2008. doi: 10.1029/2008GL034395.

L. Petitdemange, E. Dormy, and S. Balbus. Axisymmetric and non-axisymmetric magnetostrophic MRI modes. *Physics of the Earth and Planetary Interiors*, 223:21–31, Oct. 2013. doi: 10.1016/j.pepi.2013.03.003.

M. Rieutord. The dynamics of the radiative envelope of rapidly rotating stars. I. A spherical Boussinesq model. *Astronomy and Astrophysics*, 451:1025–1036, June 2006. doi: 10.1051/0004-6361:20054433.

P. H. Roberts and E. M. King. On the genesis of the Earth's magnetism. *Reports on Progress in Physics*, 76(9):096801, Sept. 2013. doi: 10.1088/0034-4885/76/9/096801.

N. Schaeffer, D. Jault, H.-C. Nataf, and A. Fournier. Turbulent geodynamo simulations: a leap towards Earth's core. *Geophysical Journal International*, 211:1–29, Oct. 2017. doi: 10.1093/gji/ggx265.

D. Shalybkov and G. Rüdiger. Non-axisymmetric instability of density-stratified taylor-couette flow. *Journal of Physics: Conference Series*, 14(1):128, 2005. URL http://stacks.iop.org/1742-6596/14/i=1/a=016.

E. A. Spiegel and J.-P. Zahn. The solar tachocline. *Astronomy and Astrophysics*, 265:106–114, Nov. 1992.

R. J. Tayler. The adiabatic stability of stars containing magnetic fields-I.Toroidal fields. *Monthly Notices of the RAS*, 161:365, 1973. doi: 10.1093/mnras/161.4.365.

J. T. Thomas and N. O. Weiss. *Sunspots and starspots*. Cambridge Astrophysics Series. Cambridge University Press, 2008.

S. A. Triana, E. Moravveji, P. I. Pápics, C. Aerts, S. D. Kawaler, and J. Christensen-Dalsgaard. The Internal Rotation Profile of the B-type Star KIC 10526294 from Frequency Inversion of its Dipole Gravity Modes. *Astrophysical Journal*, 810:16, Sept. 2015. doi: 10.1088/0004-637X/810/1/16.